International Journal of Engineering Research and Technology. ISSN 0974-3154, Volume 12, Number 11 (2019), pp. 2017-2022

Heat Transfer in a Developing Low-Amplitudes Pulsating Laminar Flow in a Square Channel

Purdin Michail Sergeevich

National Research University "Moscow Power Engineering Institute", Moscow, Russia.

ORCID: 0000-0002-5601-4845

Abstract

The article presents a methodic for the numerical simulation of heat transfer in a developing low-amplitude pulsating laminar flow in a square channel, based on the boundary layer theory. The dependences of the changes in the balk fluid temperature, the wall temperature, the heat flux on the wall, and the Nusselt number along the channel of the square cross-section are presented and analyzed, depending on the Prandtl number, amplitude and pulsation frequency.

Keywords: heat transfer, pulsations, square channel, laminar flow.

I. INTRODUCTION

Microelectronic devices used in modern computing systems and devices emit a large amount of heat. The heat flux density can reach 70 kW/m^2 on the central processors crystals surfaces [1]. This leads to the need to develop new means of heat removal with microchannel structures in which fluid flows. The small size of the channels determines the laminar flow regime.

As a method of intensification, the imposition of pulsations on the flow is sometimes considered. There are a number of works [2–13] devoted to the laws of heat transfer in a pulsating flow. An objective analysis of the papers shows that achieve significant intensification of heat transfer is impossible, and the imposition of pulsations leads to a strong increase in hydrodynamic resistance and pumping power. A significant discrepancy in the obtained values of the Nusselt number and the lack of comparisons of the results with other authors cast doubt on the results of various studies. The result depends strongly on the sequence of integration over time and the method for determining the values included in the Nusselt number, especially for amplitudes of fluid flow pulsations referred to a time average flow, $A \geq 1$. This was also noted in [9], [10]. The latter proposes four methods for determining the Nusselt number in a pulsating flow, however, none of them carries physical meaning.

There are studies of the effect of the pulsating flow on heat transfer at the entrance hydrodynamic length of the circular channel [11], [12], [13], however, there are no detailed studies of heat transfer in the pulsating laminar flow in the entrance hydrodynamic length of the square channel. Currently available research results do not give an unambiguous answer to the question of how the heat transfer changes with the change in the regime parameters of the pulsating laminar flow. Thus, conducting computational research in this area is important from a practical and theoretical point of view.

II. PROBLEM STATEMENT

The distribution of velocity components during a pulsating laminar flow of an incompressible fluid in a square channel is described by the equations of motion

$$\frac{\partial u}{\partial t}+u\frac{\partial u}{\partial x}+\upsilon\frac{\partial u}{\partial y}+w\frac{\partial u}{\partial z}=\nu\left(\frac{\partial^2 u}{\partial y^2}+\frac{\partial^2 u}{\partial z^2}\right)-\frac{1}{\rho}\frac{dp}{dx} \qquad (1)$$

and continuity

$$\frac{\partial u}{\partial x}+\frac{\partial \upsilon}{\partial y}+\frac{\partial w}{\partial z}=0, \qquad (2)$$

where p – is the pressure, t – is the time, u, υ and w – is the velocity components along the x, y and z axes, ν – is the kinematic viscosity, ρ – is the density.

This form of equations (1) and (2) corresponds to the boundary layer theory and is obtained by discarding the terms that are part of the complete Navier-Stokes equations with a small order of magnitude [14]. Since $\upsilon \wedge w << u$, there is no need to solve the momentum conservation equation for the transverse velocity components. They have some influence in solving the heat transfer equation, as well as the equations of motion (1). At Re < 100, it is impossible to neglect the solution of the equation of motion for the transverse component of the velocity, since the entrance hydrodynamic length becomes comparable or less than the height of the channel, and the transverse component of the velocity becomes comparable or greater than the longitudinal component. The research area is limited by Reynolds number in the range of 100 < Re < 2000.

For velocity, we have equations (1) and (2), which must be supplemented with the third equation, as well as the formula for finding the pressure gradient.

The pressure gradient for each section and time instant can be easily selected based on the integral continuity equation $\frac{\partial < u >}{\partial x} = 0$ (the sign < > means averaging over the section or perimeter). The method is described in detail in [15].

The second transverse velocity component can be approximately calculated using the formula $wy = \upsilon z$, first proposed R.W. Hornbeck (see [16]).

The temperature distribution in a pulsating laminar flow of an incompressible fluid in a square channel is described by the energy equation

$$\rho c_p\left(\frac{\partial T}{\partial t}+u\frac{\partial T}{\partial x}+\upsilon\frac{\partial T}{\partial y}+w\frac{\partial T}{\partial z}\right)=\lambda\left(\frac{\partial^2 T}{\partial y^2}+\frac{\partial^2 T}{\partial z^2}\right), \qquad (3)$$

where T – is the temperature, λ – is the thermal conductivity, c_p – is the heat capacity.

Axial thermal conductivity can affect heat transfer within the entrance thermal length at sufficiently low Peclet numbers Pe = RePr. Based on the range of variation of the Reynolds number, within the framework of the task, the range of variation of the Prandtl number is $0.7 \le \mathrm{Pr} \le 7$. In this case, the Peclet number varies in the range $70 < \mathrm{Pe} < 14\,000$. The boundaries of variation the region of the Prandtl number correspond to the properties for air and water under normal conditions. Most gases and liquids in a wide range of temperatures and pressures, except liquid metals, have Pr > 0.67. At small Prandtl numbers, the entrance thermal length is much less than the hydrodynamic one, therefore, in addition to axial heat conductivity, the transverse velocity components will have a significant effect on heat transfer, and the application of the boundary layer theory in this case is incorrect. For large Prandtl numbers, the entrance thermal length is much longer than the hydrodynamic one, and the results on the development of heat transfer in this case can be obtained using a simpler model for a stabilized pulsating flow.

In the dimensionless form for a pulsating flow, equations (1), (2) have the form:

$$\mathrm{S}^2\frac{\partial U}{\partial t_\omega}+U\frac{\partial U}{\partial X}+V\frac{\partial U}{\partial Y}+W\frac{\partial U}{\partial Z}=\frac{\partial^2 U}{\partial Y^2}+\frac{\partial^2 U}{\partial Z^2}+P, \qquad (4)$$

$$\frac{\partial U}{\partial X}+\frac{\partial V}{\partial Y}+\frac{\partial W}{\partial Z}=0, \qquad (5)$$

where $P=-\dfrac{d_\mathrm{h}\mathrm{Re}}{\rho<\bar{u}>}\dfrac{dp}{dx}$ – is the dimensionless pressure gradient, $\mathrm{Re}=<\bar{u}>d_\mathrm{h}/\nu$ – is the Reynolds number, $d_\mathrm{h}=h$ – is the hydraulic diameter, h – is the height of the square channel, $\mathrm{S}=d_\mathrm{h}\sqrt{\omega/\nu}$ – is the dimensionless pulsation frequency, $t_\omega = \omega t$ – is the dimensionless time; $U=u/<\bar{u}>$, $V=\upsilon\mathrm{Re}/<\bar{u}>$ and $W=w\mathrm{Re}/<\bar{u}>$ – is the dimensionless longitudinal and the transverse velocity components; $X=x/(d_\mathrm{h}\mathrm{Re})$, $Y=y/d_\mathrm{h}$ и $Z=z/d_\mathrm{h}$ – is the dimensionless longitudinal and the transverse coordinates; ω – is the circular frequency, the sign ¯ means averaging over time.

Figure 1 shows a scheme of the region for calculating the distribution of velocity components with boundary conditions. At the channel entrance, at $X=0$, a uniform velocity profile without transverse components ($U=1+A\sin\omega t$, $V = 0$, $W = 0$) is specified. This simplification is valid for Reynolds numbers Re > 100, when the thickness of the dynamic boundary layer is small compared to the height of the channel. On the wall, at $Y = Y_0$ or $Z = Z_0$, the adhesion condition is specified ($U = 0$, $V = 0$, $W = 0$). For $Y = 0$ or $Z = 0$, the symmetry condition is specified ($\dfrac{\partial U}{\partial Y}=0$ and $V = 0$ or $\dfrac{\partial U}{\partial Z}=0$ and $W = 0$). The length of the region for calculating is taken equal to two lengths of the entrance hydrodynamic length $X_0 = 0.1504$.

In practice, there is some upstream space before entering the channel. For $A > 1$ the fluid flow part of the period moves in the opposite direction and enters this space, which is a problem for the modelling of a pulsating flow associated with a lot of number of its geometric parameters. For $A > 1 \wedge A \approx 1$ at certain times, the transverse component of the velocity becomes comparable or greater than the longitudinal component of the velocity. In addition, the occurrence of secondary vibrations is possible at $A \approx 1$, since in the upstream space there occurs a counter leakage of two flows, which can lead to instability with respect to the axis of symmetry and the formation of vortices. For these cases, the model must be supplemented by equations of motion for the transverse components of the velocity. The model under consideration does not include upstream space and the possible asymmetry of the flow, therefore, the amplitude of the average velocity cross section is limited by the range $0 < A << 1$.

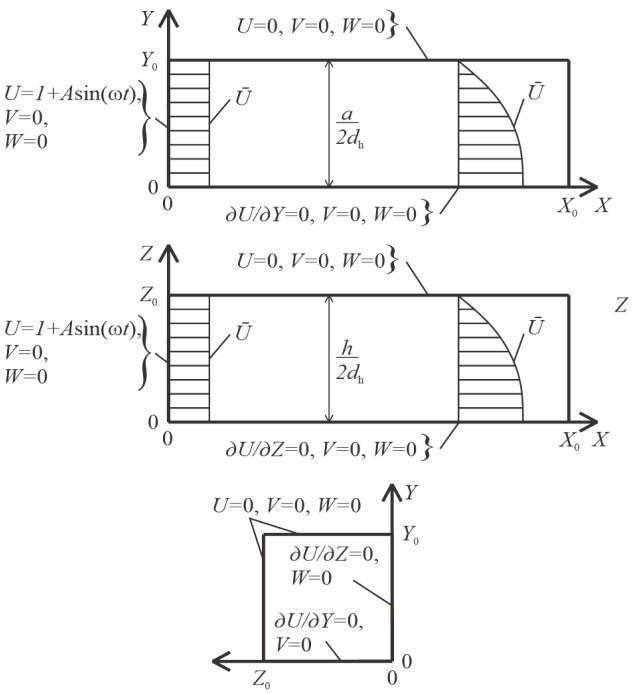

Fig. 1. Scheme of the region for calculating the distribution of velocity components.

In the dimensionless form equation (3) has the form:

$$\mathrm{Pr}\left(\mathrm{S}^2\frac{\partial \vartheta}{\partial t_\omega}+U\frac{\partial \vartheta}{\partial X}+V\frac{\partial \vartheta}{\partial Y}+W\frac{\partial \vartheta}{\partial Z}\right)=\frac{\partial^2 \vartheta}{\partial Y^2}+\frac{\partial^2 \vartheta}{\partial Z^2}, \qquad (6)$$

where $\mathrm{Pr}=\nu/a$ – is the Prandtl number, $a=\lambda/(\rho c_p)$ – is the thermal diffusivity, $\vartheta=(T-T_0)/(T_\mathrm{w}-T_0)$ – is the dimensionless fluid temperature for the first kind boundary condition on the wall, ($\vartheta=\lambda(T-T_0)/(d_\mathrm{h}q_\mathrm{w})$ – for the second kind boundary condition), T_0 – is the fluid temperature at the

channel entrance, T_w – is the wall temperature, q_w – is the heat flux on the wall.

Figure 2 shows a scheme of the region for calculating the temperature distribution with boundary conditions.

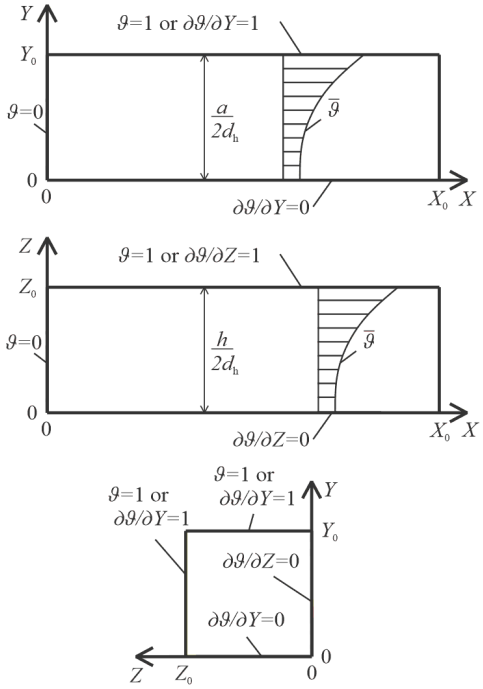

Fig. 2. Scheme of the region for calculating the temperature distribution.

III. METHODS OF NUMERICAL SOLUTION

Solutions of equations (4), (5) and (6) were found by the finite difference method. The time derivative is approximated using an implicit unconditionally stable two-layer time difference scheme. For the approximation of the convective part of the motion equation, the "against flow" scheme was used, since even for $A < 1$ and $S > 1$ return flows near the wall can occur [17], which can lead to instability of the solution and incorrect results. The calculations results of hydrodynamics with return flows were not applied when solving the energy equation, for the convective part of which an implicit two-layer scheme with the first order was applied. To approximate the first derivatives in the continuity equation, an implicit two-layer scheme with the first accuracy order is used. To approximate the second derivatives of equations (4) and (6), a central-difference scheme with a second accuracy order is used.

To solve the obtained systems of linear equations, the Gauss-Seidel method was applied. A program was written that implements computations on a video card using the C ++ AMP library. The number of partitions uniform along the axes, equal to 64x32x32x256 along the XxYxZxt_ω, was selected by sequential doubling and control of the results obtained.

Upon completion of the calculation, the time-average values of the averaged perimeter heat flux on the walls $<\overline{Q}>=\dfrac{\int_0^{2\pi}\left(\int_0^{Z_0}\left(\dfrac{\partial\vartheta}{\partial Y}\right)_{Y=Y_0}dZ+\int_0^{Y_0}\left(\dfrac{\partial\vartheta}{\partial Z}\right)_{Z=Z_0}dY\right)dt_\omega}{2\pi\left(Y_0+Z_0\right)}$, the balk fluid temperature $\overline{\vartheta}_b=\int_0^{2\pi}\int_0^{Z_0}\int_0^{Y_0}\vartheta U dY dZ dt_\omega \Big/ 2\pi Y_0 Z_0 <\overline{U}>$, the wall temperature

$$\overline{\vartheta_w}=\int_0^{2\pi}\left(\int_0^{Z_0}\vartheta_{Y=Y_0}dZ+\int_0^{Y_0}\vartheta_{Z=Z_0}dY\right)dt_\omega \Big/ 2\pi\left(Y_0+Z_0\right)$$

and the Nusselt number $\mathrm{Nu}=\dfrac{<\overline{Q}>}{\overline{\vartheta_w}-\overline{\vartheta_b}}$ were determined.

Integration over the channel cross section is carried out by the Simpson method, and in time by the trapezoid method. The integration accuracy order is not inferior to the differential equations difference approximation accuracy order, which allows the efficient use of machine resources.

IV. RESULTS

To date, studies of heat transfer in a developing pulsating laminar flow in a square channel by experimental or analytical methods have not been carried out. The program work can be verified only by comparison with the Wibulswas research results [18] for a developing stationary flow, setting A = 0. Figure 3 shows the results of calculations in the program. It can be seen that the Nusselt number averaged over the channel length correlates well with the experimental data.

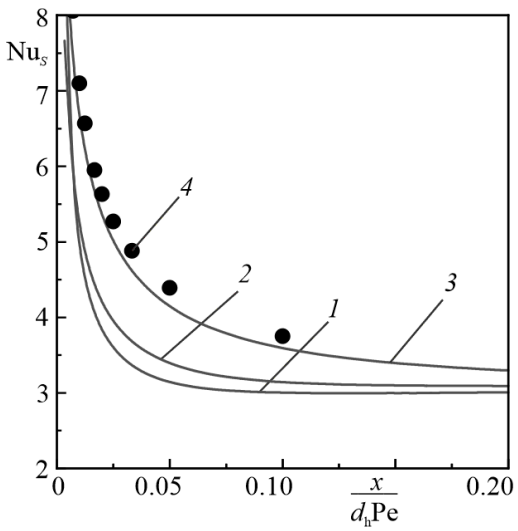

Fig. 3. Change in the Nusselt number along the length of the channel during a developing stationary flow. *1* – for the first kind boundary condition on the wall, *2* – for the second kind boundary condition, *3* – the Nusselt number averaged over the channel length for the first kind boundary condition, *4* – experimentally obtained in [18] the Nusselt number averaged over the channel length for the first kind boundary condition.

Figure 4 shows the change of the balk fluid temperature and the averaged perimeter heat flux on the wall, relatively to their stationary values, for the first kind boundary condition on the wall. In the quasi-stationary mode of pulsations (as $S \to 0$), the ratio of the heat flux on the wall to its stationary value decreases along the entire hydrodynamic length. At sufficiently high thermal frequencies $S_T = S\sqrt{Pr}$, a minimum of heat flux near the entrance of the channel can be observed. The distance to it decreases with increasing Prandtl number and pulsation frequency, since there is a decrease in the heat wavelength in the flowing fluid $X_T \sim 1/S_T$. An increase of the amplitude leads to an increase of the amplitude of thermal pulsations and an even greater decrease in the heat flux near the inlet (by 40% for A = 2/3, S = 8, Pr = 0.7). The balk fluid temperature $\overline{\vartheta}_b$ changes by no more than 5 % in the studied operating parameters range.

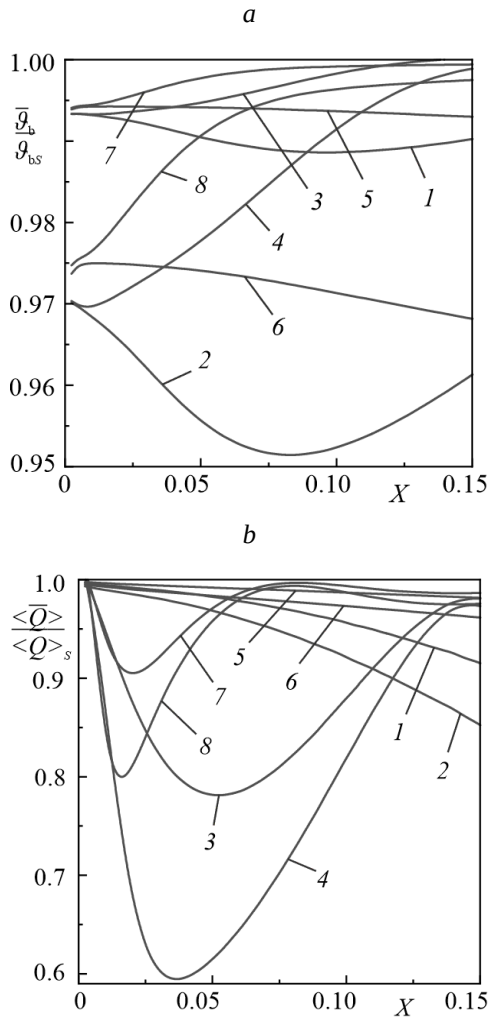

Fig. 4. Change of the balk fluid temperature (*a*) and the heat flux on the wall (*b*) for the first kind boundary condition on the wall; *1* – A = 1/3, S = 1, Pr = 0.7; *2* – A = 2/3, S = 1, Pr = 0.7; *3* – A = 1/3, S = 8, Pr = 0.7; *4* – A = 2/3, S = 8, Pr = 0.7; *5* – A = 1/3, S = 1, Pr = 7; 6 – A = 2/3, S = 1, Pr = 7; 7 – A = 1/3, S = 8, Pr = 7; *8* – A = 2/3, S = 8, Pr = 7.

Figure 5 shows the change of the balk fluid temperature and the wall temperature, relatively to their stationary values, for the second kind boundary condition. In the quasistationary regime of pulsations, the average wall temperature over the cross section increases significantly along the entrance hydrodynamic length (by 23% for A = 2/3, S = 1, Pr = 0.7 and X = 0.15). As well as for the first kind boundary condition on the wall, with an increase in the thermal frequency of the pulsations, a minimum of the wall temperature appears, which approaches the entrance. With an increase in the amplitude of pulsations, the effect on thermal quantities increases. The balk fluid temperature changes by no more than 3.5% in the studied operating parameters range. It is seen that in all modes $\overline{\vartheta}_b$ has the smallest value at the entrance to the channel and approaches a stationary value when moving away from it. The greatest influence on it is exerted by the amplitude of the pulsations and the Prandtl number, and the dimensionless frequency of the pulsations has a negligible effect.

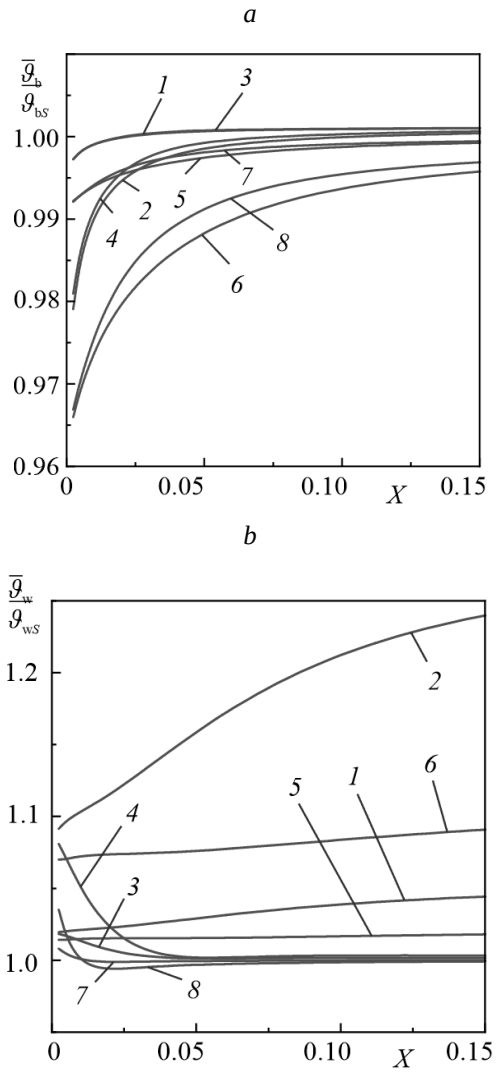

Fig. 5. Change of the balk fluid temperature (*a*) and the wall temperature (*b*) for the second kind boundary condition on the wall; *1* – A = 1/3, S = 1, Pr = 0.7; *2* – A = 2/3, S = 1, Pr = 0.7; *3* – A = 1/3, S = 8, Pr = 0.7; *4* – A = 2/3, S = 8, Pr = 0.7; *5* – A = 1/3, S = 1, Pr = 7; 6 – A = 2/3, S = 1, Pr = 7; 7 – A = 1/3, S = 8, Pr = 7; *8* – A = 2/3, S = 8, Pr = 7.

As a result of the calculations, a change of the Nusselt number along the channel length was obtained (see Fig. 6). A significant difference from the pulsating flow in a flat channel or round pipe is the absence of pronounced fluctuations in the Nusselt number along the length caused by the movement of the heat wave in the flowing fluid. At Pr = 7 and S = 8, no more than one minimum or maximum can be observed. With a decrease S, Pr or (and) an increase in the amplitude of pulsations, a significant decrease in the Nusselt number occurs. One can notice a significant correlation between the change in the Nusselt number and the change in the heat flux on the wall for the first kind boundary condition on the wall and the change in the temperature of the wall for the second kind boundary condition.

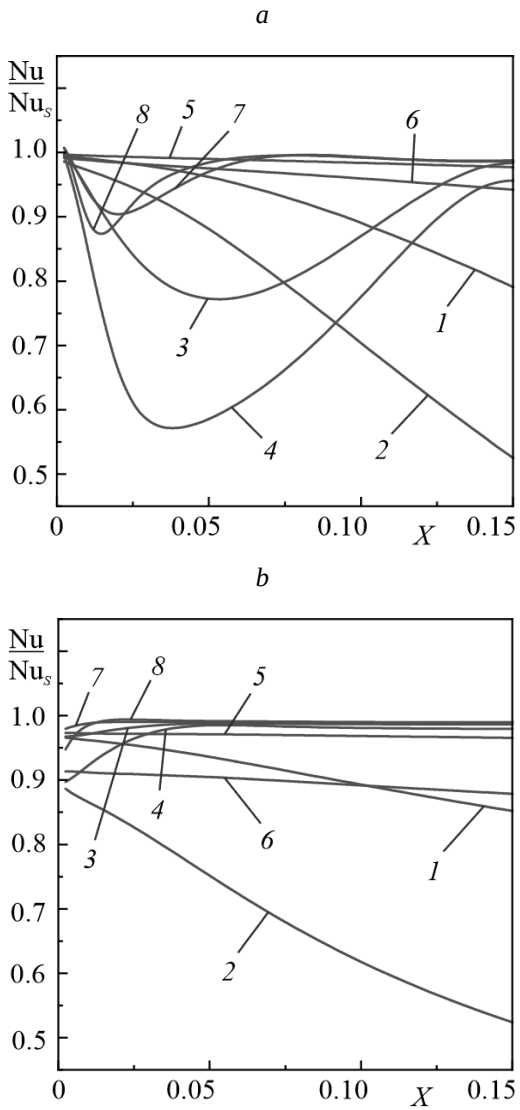

Fig. 6. The ratio of the Nusselt number to its stationary value. *a* – for the first kind boundary condition on the wall, *b* – for the second kind boundary condition on the wall; *1* – *A* = 1/3, S = 1, Pr = 0.7; *2* – *A* = 2/3, S = 1, Pr = 0.7; *3* – *A* = 1/3, S = 8, Pr = 0.7; *4* – *A* = 2/3, S = 8, Pr = 0.7; *5* – *A* = 1/3, S = 1, Pr = 7; 6 – *A* = 2/3, S = 1, Pr = 7; 7 – *A* = 1/3, S = 8, Pr = 7; *8* – *A* = 2/3, S = 8, Pr = 7.

V. CONCLUSION

A mathematical model and a technique for numerical modelling of heat transfer in a developing laminar pulsating flow with low amplitudes in a square channel have been developed.

In the studied operating parameters region for the first and the second kind boundary conditions on the wall, no significant effect of fluctuations in fluid flow on the balk fluid temperature was found. An increase in the amplitude of pulsations leads to an increase in the influence of pulsations on heat transfer. In the quasi-stationary mode of pulsation, the Nusselt number decreases along the length of the channel.

For the first kind boundary condition in the high-frequency pulsation regime, the heat flux near the entrance to the channel decreases significantly, and approaches the stationary value at a distance from the entrance, which leads to a decrease in the Nusselt number near the entrance to the channel.

For the second kind boundary condition, with an increase in the pulsation frequency, the change in the wall temperature along the length of the channel approaches the dependence for a stationary flow, therefore, the Nusselt number also approaches the stationary one.

ACKNOWLEDGMENT

This work was supported by the Ministry of Science and Higher Education of the Russian Federation, grant No. MK-2636.2018.8.

REFERENCES

[1] October 2018, “8th and 9th Generation Intel Core Processor Families and Intel Xeon E Processor Family Datasheet”, Intel Corporation, Doc. No. 337344-002.

[2] AI-Haddad A.A., AI-Binally N., 1989, “Prediction of heat transfer coefficient in pulsating flow”, Int. J. Heat and Fluid Flow, 10(2), pp. 131–133.

[3] Siegel R., Perlmutter M., 1962, “Heat transfer for pulsating laminar duct flow”, J. Heat Transfer, 84, pp. 111–122.

[4] Persoons T., Saenen T., Van Oevelen T., Baelmans M., 2012, “Effect of flow pulsation on the heat transfer performance of a minichannel heat sink”, J. Heat Transfer., 134, pp. 1–7.

[5] Nandi T.K., Chattopadhyay H., 2013, “Numerical investigations of simultaneously developing flow in wavy microchannels under pulsating inlet flow condition”, Int. Com. Heat Mass Transfer., 47, pp. 27–31.

[6] Mehta B., Khandekar S., 2015, “Local experimental heat transfer of single-phase pulsating laminar flow in a square mini-channel” Int. J. Thermal Science, 91, pp. 157–166.

[7] Yuan H., Tan S., Wen J., Zhuang N., 2016, “Heat

transfer of pulsating laminar flow in pipes with wall thermal inertia", Int. J. Thermal Science, 99, pp. 152–160.

[8] Blythman R., Persons T., Jeffers N., Murray D.B., 2019, "Heat transfer of laminar pulsating flow in a rectangular channel" Int. J. Heat Mass Transfer, 2019, 128, pp. 279–289.

[9] Hemida H.N., Sabry M.N., Abdel-Rahim A., Mansour H., 2002, "Theoretical analysis of heat transfer in laminar pulsating flow", Int. J. Heat Mass Transfer, 45, pp. 1767–1780.

[10] Guo Z., Sung H.J., 1997, "Analysis of the Nusselt number in pulsating pipe flow", Int. J. Heat Mass Transfer, 40, pp. 2486–2489.

[11] Cho Y.W., Hyun J.M., 1990, "Numerical solutions of pulsating flow and heat transfer characteristics in a pipe", Int. J. Heat and Fluid Flow, 11(4), pp. 321–330.

[12] Kim S.Y., Kang B.H., Hyun J.M., 1993, "Heat transfer in the thermally developing region of a pulsating channel flow", Int. J. Heat Mass Transfer, 36(17), pp. 4257–4266.

[13] Chattopadhyay H., Durst F., Ray S., 2006, "Analysis of heat transfer in simultaneously developing pulsating laminar flow in a pipe with constant wall temperature", Int. Comm. in Heat and Mass Transfer, 33, pp. 475–481.

[14] Schlichting H., 1965, "Grenzschicht-Theorie", Karlsruhe, C. Braun.

[15] Purdin M.S., 2019, "Developing low-amplitude pulsating laminar flow in a flat channel", IJERT, 12(4), pp. 570–578.

[16] Hornbeck R.W., 1973, "Numerical marching techniques for fluid flows with heat transfer", NASA, SP-297.

[17] Valueva E.P., Purdin M.S., 2015, "The pulsating laminar flow in a rectangular channel", Thermophysics and Aeromechanics, 22(6), pp. 733–744.

[18] Wibulswas P., 1966, "Laminar-flow heat-transfer in non-circular ducts", London, 150 p.